High-resolution observations of temperature-dependent magnetic domain structures within Ga$_x$Mn$_{1-x}$As by Lorentz microscopy

Akira Sugawara,[1,*] T. Akashi,[2,†] P. D. Brown,[3] R. P. Campion,[4] T. Yoshida,[2] B. L. Gallagher,[4] and A. Tonomura[1,2]

[1]*Initial Research Project, Okinawa Institute of Science and Technology, c/o Hitachi Advanced Research Laboratory, Akanuma 2520, Hatoyama, Saitama 350-0395, Japan*

[2]*Advanced Research Laboratory, Hitachi Ltd., Akanuma 2520, Hatoyama, Saitama 350-0395, Japan*

[3]*School of Mechanical, Materials & Manufacturing Engineering, University of Nottingham, University Park, Nottingham NG7 2RD, United Kingdom*

[4]*School of Physics and Astronomy, University of Nottingham, University Park, Nottingham NG7 2RD, United Kingdom*

The observation of magnetic domain structures within an in-plane magnetized Ga$_x$Mn$_{1-x}$As dilute magnetic semiconductor on the submicronmeter scale by Lorentz microscopy is described. A micrometer-scale domain substructure is found to be characteristic of the micromagnetics of the Ga$_x$Mn$_{1-x}$As sample. Due to the competition of temperature-dependent biaxial and uniaxial anisotropy, conventional zigzag and unusual segmented domain structures are identified, with the latter exhibiting spontaneous reorganization with varying temperature. The experimental results are compared with micromagnetic simulations.

Gallium manganese arsenide is a III-V dilute magnetic semiconductor[1] (DMS) and a promising model system for future spintronic devices because the magnetic functionality can be integrated within high-speed GaAs-based device structures. When developing device structures for spintronic applications, it is important to understand the micromagnetics of the DMS domain structures. In-plane magnetized Ga$_x$Mn$_{1-x}$As(001) layers are known to exhibit the biaxial magnetocrystalline anisotropy of the [100] and [010] easy axes at low temperature, but the uniaxial anisotropy of the [110] easy axis at high temperature.[2] Welp *et al.* reported that the [100] and [010] easy axes gradually rotate toward [110] with increased temperature, and emergence to the [110] easy axis is described as second-order transition with a certain transition temperature around $(1/2)T_c$, (where T_c is the Curie temperature).[3] It is also suggested that the transition temperature varies with the ratio of the biaxial and uniaxial magneticrystalline anisotropy constants (K_c and K_u, respectively), which depends on the specimens.[4]

Although magnetic anisotropy has been extensively studied by magnetization-field (M-H) loop measurements, a limited number of studies have been reported on the direct observation of in-plane magnetized Ga$_x$Mn$_{1-x}$As DMS domain structures, e.g., using magneto-optical microscopy with a garnet film as a Faraday indicator,[3] or scanning Hall probe microscopy.[5] These investigations have demonstrated that 90° walls are dominant for $T < (1/2)T_c$, whilst 180° walls are dominant for $(1/2)T_c < T < T_c$, showing correlation with the magnetic anisotropy revealed by macroscopic M-H loop measurements.[3] The specimens with the out-of-plane easy axis have been also observed.[6,7]

Domain structures within an electron transparent sample foil may be observed directly with spatial resolution on the order of tens of nanometers using Lorentz microscopy.[8] The process of image formation is based on the interference of electron waves, deflected in different directions in response to the in-plane magnetization components within each domain, and hence can provide direct information on in-plane magnetic structures including Néel-type walls that may not be correctly observed by the methods detecting the stray field employed in the previous studies. In spite of these advantages, Lorentz electron microscopy has not been applied as yet to the study of DMS alloys. One reason for this is very small magnetizations (M_s), typically 0.02 T for Ga$_x$Mn$_{1-x}$As. The phase shift of transmitted electrons through a magnetized material is proportional to the product of M_s and the foil thickness. Accordingly, a Ga$_x$Mn$_{1-x}$As foil a hundred times thicker than a corresponding Fe foil (M_s=2.0 T) would be needed to obtain the same spatial phase gradient. The image contrast due to such small phase gradients in thick foils may also become masked by fluctuations of the electrostatic phase shift, due to specimen thickness variations and inelastic scattering. Since the previous observation suggested a domain size larger than tens of micrometers for Ga$_x$Mn$_{1-x}$As thin films,[3] this places a significant constraint on the process of sample preparation for Lorentz microscopy.

For the purpose of this experiment, a designed Ga$_{0.96}$Mn$_{0.04}$As (500 nm)/GaAs (1 nm)/AlAs (50 nm)/buffer GaAs (100 nm) multilayer was deposited onto a GaAs(001) wafer using molecular beam epitaxy.[9] The AlAs intermediate layer was incorporated to provide an etch stop. The GaAs substrate was removed by mechanical polishing, followed by selective chemical etching[10] to provide a uniformly thick sample foil with a wide field of view on the length scale of 100 μm. This particular as-grown Ga$_x$Mn$_{1-x}$As specimen was found to have an M_s value of 0.024 T at 4.2 K and a T_c of approximately 60 K by superconducting quantum interference device (SQUID) measurements. The dominant magnetic anisotropy was found to be biaxial at 4.2 K, and uniaxial at 50 K.

The in-plane magnetic domain structure was observed under zero-field conditions as a function of temperature by Lorentz imaging in the Fresnel mode, using the 1-MeV cold FEG transmission electron microscope TEM to minimize incoherent scattering.[11] The specimen was located out of the pole-piece gap of the microscope objective lens, to allow the
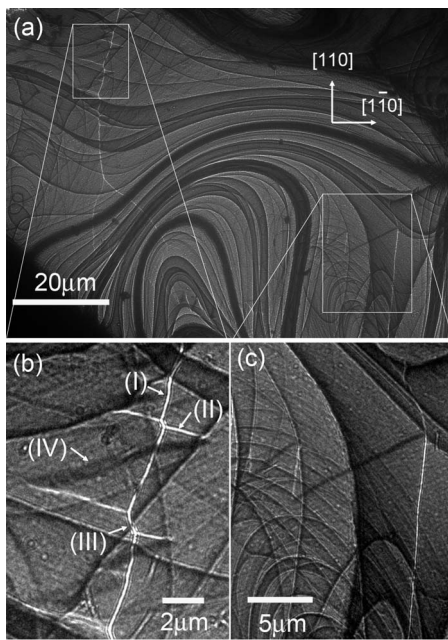
FIG. 1. Lorentz micrographs of a 500-nm-thick $Ga_{0.96}Mn_{0.04}As$ film recorded at 12 K. (a) A low-magnification image; and (b), (c) enlarged images for the regions framed by white rectangles.
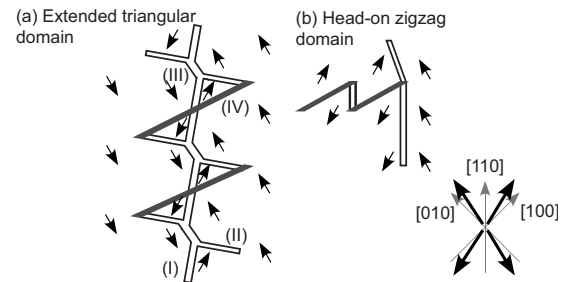

FIG. 2. Schematic diagrams of the domain walls and moment configurations. (a) Extended triangular domain shown in Fig. 1(b); and (b) head-on 180° domain shown in Fig. 1(c). The condition of stable magnetization M deviates between [100] and [110] as a result of the competition between K_c and K_u.

observation of the micromagnetic structures under conditions of residual magnetic field smaller than 0.1 mT perpendicular to the film plane. A temperature range at the sample between 8 and 60 K was established using a helium-cooled specimen holder, with the temperature deviation between the specimen and the readout estimated to be within 5 K.

Figure 1(a) shows a low-magnification, overfocused ($\Delta f \sim 12$ mm) Lorentz image of the semi-self-supporting $Ga_{0.96}Mn_{0.04}As/GaAs/AlAs$ trilayer plan-view sample at 12 K as developed on cooling from the paramagnetic state under zero field. The specimen was found to be almost free of visible structural defects,[12] with the image contrast being dominated by crystal bend contours. Contrast from the domain walls could, however, be distinguished easily by examining the variation of contrast as a function of defocus. Typical examples of domain wall contrast, framed by white rectangles in Fig. 1(a) are enlarged and presented in Figs. 1(b) and 1(c).

The segmented domain wall structure shown in Fig. 1(b) and summarized schematically in Fig. 2(a) takes the form of triangular domains extending from a central kinked domain wall. To the best of our knowledge, this type of structure has not been identified within any other material to date. For this Lorentz deflection geometry, the image contrast became stronger whilst the fringe spacing became shorter as the relative angle of the moments in the neighboring domains across the wall increased. Four different types of local domain wall contrast have been identified within the image. The result indicates that the symmetry was lowered, i.e., exactly quadratic 90° walls did not occur even at 10 K due to the influence of uniaxial anisotropy. Type-I and type-II walls are considered to be 90°-like domain walls nearly parallel to [110] and [1$\bar{1}$0], respectively. Type-I walls exhibit stronger contrast than type-II walls because the relative angle between

the magnetic moments within neighboring domains, either side of a type-I wall, is larger, suggesting that the stable magnetization deviate from the exact [100] and [010] directions toward [110], although the deviation angle was not determined precisely in the present experiment. In contrast, the type-III walls are considered to be 180° walls, in view of their very strong contrast and the association of narrow Fresnel interference fringes. However, type-III walls appeared only as short segments within these segmented wall structures, suggesting them to be energetically unfavorable. Type-IV walls exhibited inverted contrast to other types of walls, indicating an inversion of the rotational direction of magnetization across this wall type. The combination of domain walls of types I, II, and III act to produce a vortex, while intersecting type-II and -IV domain walls act to produce an antivortex, with both segments being composed of 90°-like walls with Bloch lines at the center.[13]

Even though most of the local domain walls are 90°-like, with energetically disadvantaged 180° wall components being observed only as short segments, from a macroscopic point of view, it is considered that this type of segmented domain structure behaves overall as a 180° wall because the magnetizations either side of the composite domain wall are antiparallel. This characteristic feature is reminiscent of the nature of cross-tie walls[13] across which the total energy similarly decreases by a replacement of 180° walls with combined 90° walls at the tie lines, with the inducement of a continuous spatial transition of the moments in between the tie lines ensuring that the moments far from each wall are maintained in an antiparallel configuration. It is noted that the gradual transition of moments associated with the cross-tie wall structure originates from weak anisotropy. The significant feature of the present segmented domain wall structure is that a much more abrupt transition is observed due to the strong anisotropy.

A second type of feature, more typical of the domain wall structures identified within the present specimen, is illustrated in Fig. 1(c) and schematically in Fig. 2(b), being an example of a simple head-on zigzag wall combined with a 90°-like wall. Such zigzag domain wall structures tended to remain at the same locations upon sample thermal cycling and hence are thought to be influenced by the effects of local pinning, although explicit contrast due to structural defects was not observable at the zigzag junctions.
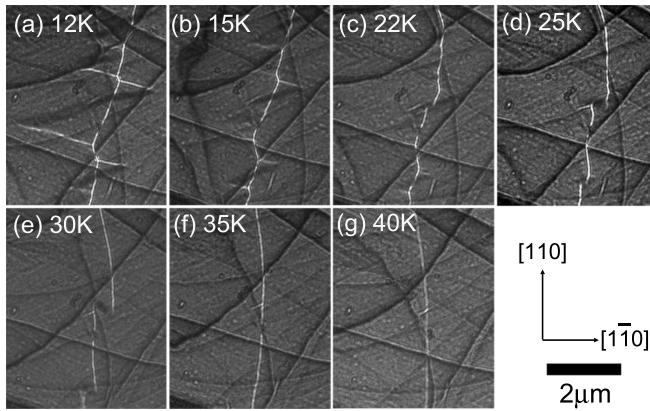
FIG. 3. Lorentz micrographs of a segmented wall as a function of temperature under zero-field conditions. The specimen temperature was raised from 12 to 40 K.
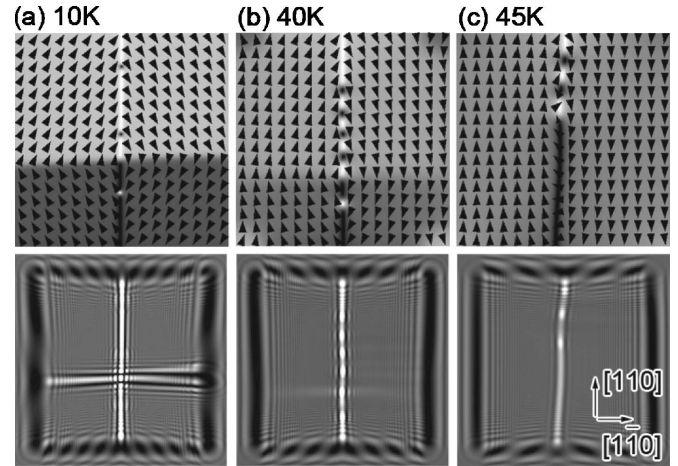

FIG. 4. Magnetic domains simulated by the LLG method and corresponding underfocus images ($\Delta f \sim 50$ mm) calculated by using the Fresnel propagator method. The micromagnetic parameters used for the simulation are (a) $T=10$ K, $M_s=2.31\times10^{-2}$ T, $A=1.4$ pJ/m, $K_c=1.08\times10^3$ J/m^3, $K_u=4.98\times10^2$ J/m^3; (b) $T=40$ K, $M_s=1.61\times10^{-2}$ T, $A=0.7$ pJ/m, $K_c=2.74\times10^2$ J/m^3, and $K_u=2.32\times10^2$ J/m^3; and (c) $T=45$ K, $M_s=1.36\times10^{-2}$ T, $A=0.54$ pJ/m, $K_c=1.44\times10^2$ J/m^3, and $K_u=1.63\times10^2$ J/m^3.

Significant differences between the segmented (extended triangular) and zigzag domain wall structures were observed when the specimen temperature was varied. Figure 3 illustrates the change of contrast exhibited by the segmented domain structure of Figs. 1(b) and 2(a). The domain structure spontaneously reorganized with a raising of the temperature, even under conditions of zero field. The image contrast became modified in response to the wall motion, with rotation of the magnetic moments within each domain and consequent modification of the angle of electron deflection due to a decay of the temperature-dependent saturation magnetization, although we could not separate each contribution quantitatively in the present study. The result suggests that the segmented wall is a metastable state, which is caused to compensate misalignment of domain walls from [110] probably due to wall pinning. When the temperature was increased from 12 K [Fig. 3(a)], the segmented domain walls clearly observable in the beginning gradually contracted [Figs. 3(b) and 3(c)] and almost disappeared at 25 K [Fig. 3(d)], becoming transformed into a zigzag and then a straight domain wall nearly parallel to [110] at 30 K [Fig. 3(e)] and 35 K and above [Figs. 3(f) and 3(g)], respectively. The domain contrast disappeared above 48 K at $\Delta f = -80$ mm. The corresponding saturation magnetization was determined to be 0.012 T by correlated SQUID measurements. Conversely, the zigzag and 90° walls in Figs. 1(c) and 2(b) did not exhibit significant change upon thermal cycling (results not shown here). A gradual rotation of the magnetic moment within each domain, in this instance, most likely resulted in a minimization of energy without the need for any significant changes in the domain wall shape. The 90°-type walls with reduced angle, i.e., small-angle walls, were frequently observed above 40 K, although their contrast became weakened with increasing temperature. Lorentz microscopy was thus confirmed to be sensitive for detection of small-angle domain walls associated with the spin-reorientation transition within DMS Ga$_x$Mn$_{1-x}$As alloys.[2–4]

The magnetocrystalline anisotropy of the Ga$_x$Mn$_{1-x}$As is also known to be sensitive to stress state of specimens.[14] The heteroepitaxial strain was considered to be partially relieved after the GaAs substrate was removed in the present experi-

ment. Also strain due to the specimen bend may influence the anisotropy. We observed frequently that the walls tend to be curved where the bend contour takes irregular shapes. The nonuniform strain thus produced wall pinning sites. However, we confirmed that the magnetic anisotropy was not modified significantly even after the substrate was removed. We performed *in situ* magnetization experiment in the microscope. The wall motion occurred around −20 Oe when the field was applied parallel to [100] at 10 K. The field magnitude was comparable to reversal field determined by SQUID.[15]

To help validate the assignments of these experimentally observed features, Landau-Lifshitz-Gilbert (LLG) micromagnetic simulations[16] and Lorentz image simulations were performed to confirm the temperature-dependent contrast of the domain wall structures as a function of the micromagnetic parameters. Saturation magnetization M_s was measured as a function of temperature by SQUID. The temperature-dependent exchange stiffness A was derived from Goennenwein *et al.*'s experimental result obtained by spin-wave resonance, assuming a $T^{3/2}$ dependency.[17] The cubic (in-plane biaxial) anisotropy constant K_c and the uniaxial constant K_u were derived from their magnetization dependence, as reported by Wang *et al.*.[4] The LLG simulations were performed for platelets of dimension $4000\times4000\times500$ nm^3 with the edge directions parallel to [110] and [1$\bar{1}$0] at (a) 10, (b) 40, and (c) 45 K, respectively (Fig. 4). All the walls obtained in the simulations were of symmetric Néel type, although we did not determine the type of the wall from the Lorentz images. The direction of stable magnetization was found to approach [110], with K_u dominant at high temperature, while approaching [100] and [010] with K_c dominant at low temperature. The direction of magnetization was aligned parallel to the magnetocrystalline easy direction, determined

by K_c/K_u, even at the platelet edges. The contribution of the stray field energy is relatively weak when the magnetization is small, as in the case of $Ga_xMn_{1-x}As$. Accordingly, it is evident that the micromagnetic structure of the $Ga_xMn_{1-x}As$ system is dominated by the magnetocrystalline anisotropy. At 10 K the platelets adopted a vortex structure comprising 90°-like domain walls [Fig. 4(a)]. The magnetization within each domain deviated by approximately 12° from $\langle 100 \rangle$ towards [110] due to the weak uniaxial anisotropy. The relative angle of the moments across such 90°-like domain walls was found to be slightly larger for walls parallel to [110] than [1$\bar{1}$0], i.e., for conditions of lowered symmetry. When K_c and K_u are comparable at 40 K, the magnetization within each domain across the boundary wall deviated by approximately 17° from [110] toward $\langle 100 \rangle$ due to the weak biaxial anisotropy. The difference between [110] and [1$\bar{1}$0] walls becomes clearly visible [Fig. 4(b)]. In contrast, 180°-like walls parallel to [110] was produced for 45 K, where $K_u > K_c$

Having established that the conditions of stable magnetization could be modeled, the phase modulation of the transmitted electron wave at the exit surface of the specimen was then calculated as a consequence of the Lorentz beam deflection, using the Fresnel propagator method. The simulated underfocus Lorentz image at 10 K corresponding to 90°-like walls parallel to both [110] and [1$\bar{1}$0] [Fig. 4(a)] shows that the [110] wall exhibits stronger contrast, with a shorter period of interference fringes. This is consistent with the experimental observations of differing [110] and [1$\bar{1}$0] wall contrast. In the simulated underfocus Lorentz image at 40 K, the magnetization distribution across the small-angle [1$\bar{1}$0] wall is profiled as weaker wall contrast in Fig. 4(b). It is also noted that the vortex-antivortex pairs on the straight wall segment also give strong contrast. In the simulated image for 45 K, we cannot find contrast associated with the [1$\bar{1}$0] walls. Thus, a condition of lowered symmetry is directly confirmed by the Lorentz contrast, as observed in the experiment.

*Present address: Advanced Research Laboratory, Hitachi Ltd. Electronic address: akira.sugawara.ne@hitachi.com

†Also at the Hitachi High-tech Fielding Corporation.

[1] H. Ohno, A. Shen, F. Matsukura, A. Oiwa, A. Endo, S. Katsumoto, and H. Iye, Appl. Phys. Lett. **69**, 1849 (1996); H. Ohno, Science **381**, 951 (1998).

[2] D. Hrabovsky, E. Vanelle, A. R. Fert, D. S. Yee, J. P. Redoules, J. Sadowski, J. Kanski, and L. llver, Appl. Phys. Lett. **81**, 2806 (2002).

[3] U. Welp, V. K. Vlasko-Vlasov, X. Liu, J. K. Furdyna, and T. Wojtowicz, Phys. Rev. Lett. **90**, 167206 (2003).

[4] K.-Y. Wang, M. Sawicki, K. W. Edmonds, R. P. Campion, S. Maat, C. T. Foxon, B. L. Gallagher, and T. Dietl, Phys. Rev. Lett. **95**, 217204 (2005).

[5] A. Pross, S. Bending, K. Edmonds, R. P. Campion, C. T. Foxon and B. J. Gallagher, J. Appl. Phys. **95**, 7399 (2004); **95** 3225 (2004).

[6] T. Shono, T. Hasegawa, T. Fukumura, F. Matsukura, and H. Ohno, Appl. Phys. Lett. **77**, 1363 (2000).

[7] A. Dourlat, C. Gourdon, V. Jeudy, C. Testelin, L. Thevenard, and A. Lemaitre, Phys. Status Solidi C **3**, 4074 (2006).

[8] A. K. Petford-Long and J. N. Chapman, in *Magnetic Microscopy of Nanostructures*, edited by H. Hopster and H. P. Oepen (Springer-Verlag, Berlin, 2004), p. 67.

[9] R. P. Campion, K. W. Edmonds, L. X. Zhao, K. Y. Wang, C. T. Foxon, B. L. Gallagher., and C. R. Staddon, J. Cryst. Growth **247**, 42 (2003).

[10] Rong Zhao, Wai Shing Lau, Tow Chong Chong, and Ming Fu Li, Jpn. J. Appl. Phys., Part 1 **35**, 22 (1996).

[11] T. Kawasaki, T. Yoshida, T. Matsuda, N. Osakabe, A. Tonomura, I. Matsui, and K. Kitazawa, Appl. Phys. Lett. **76**, 1342 (2000).

[12] M. W. Fay, Y. Han, P. D. Brown, K. W. Edmonds, K. Wang, B. L. Gallagher, R. P. Campion, and C. T. Foxon, Philos. Mag. Lett. **86**, 395 (2006).

[13] A. Hubert and R. Schäfer, *Magnetic Domains: The Analysis of Magnetic Microstructures* (Springer, Berlin, 1998).

[14] M. Sawicki, F. Matsukura, A. Idziaszek, T. Dietl, G. M. Schott, C. Ruester, C. Gould, G. Karczewski, G. Schmidt, and L. W. Molenkamp, Phys. Rev. B **70**, 245325 (2004).

[15] See EPAPS Document No. E-PRBMDO-75-R23724 for correlation between in-situ observation of domain motion in the electron-transparent specimen under magnetic field and an ex-situ SQUID loop of $Ga_{0.96}Mn_{0.04}As$ as deposited on the GaAs wafer. For more information on EPAPS, see http://www.aip.org/pubservs/epaps.html.

[16] M. R. Scheinfein, ʟʟɢ Micromagnetics Simulator, version 2.59a (2006).

[17] S. T. B. Goennenwein, T. Graf, T. Wassner, M. S. Brandt, M. Stutzmann, J. B. Philipp, B. Gross, M. Krieger, K. Zürn, P. Ziemann, A. Koeder, S. Frank, W. Schoch, and A. Waag, Appl. Phys. Lett. **82**, 730 (2003).